Laser line scanner aptitude for the measurement of Selective Laser Melting parts

Optics and Lasers in Engineering Vol. 138, March 2021, 106406
https://doi.org/10.1016/j.optlaseng.2020.106406

E. Cuesta[a], S. Giganto[b], B.J. Alvarez[a], J. Barreiro[b], S. Martínez-Pellitero[b], V. Meana[a]

[a] *Department of Construction and Manufacturing Engineering, University of Oviedo, Campus de Gijon, 33204 Gijon, Spain*
[b] *Department of Manufacturing Engineering, University of Leon, Escuela de Ingenierias Industrial e Informatica, 24071 Leon, Spain*

Abstract
When looking for any metrological verification of parts manufactured by metal laser printing with optical equipment, it is necessary to ensure the traceability of the measurements that can be obtained. The difficulty of this process lies in the fact that these measurements are obtained on point clouds captured from surfaces with high form errors and poor surface finishes, even when this type of surface usually undergoes processes to improve the surface finish, such as sandblasting. This research focuses precisely on the analysis of the metrological suitability of a laser line scanner (laser triangulation sensor) on parts manufactured by Selective Laser Melting (SLM).

The study starts from the design of a test part specifically oriented to the printing process with SLM metal powder bed. This test part was printed in 17-4PH stainless steel and then sandblasted. The test part was measured in a Coordinate Measuring Machine (CMM), obtaining reference GD&T values. The measurement was carried out under pre-sandblasting ("as built") and post-sandblasting conditions, thus providing interesting information about the erosion rate of this post process. A state-of-the-art laser sensor was employed for the metrological comparison, mounted on the same available CMM that was used for contact measurements.

In this research three analyses were carried out: the quality of 3D metal printed parts with respect to CAD model, the effect of the sandblasting post-process, and the accuracy of the measurements obtained with the laser line sensor. In addition, this work conducts an in-depth study about the influence of point cloud treatment and filtering procedures, by comparing the filtering methods applied by different reverse engineering software packages. The study leads to the conclusion that filters based on the standard deviation of the point cloud are the best candidates in order to obtain laser measurements closer to the contact measurements.

Keywords
Selective Laser Melting (SLM); laser line scanner; 3D metrology

1. Introduction

Non-contact optical measurement and reverse engineering techniques are increasingly used for the measurement and verification of parts obtained by additive manufacturing techniques. In the case of Selective Laser Melting (SLM), where it is intended to generate functional parts in small batches or even unique, the use of these non-contact inspection techniques is even more interesting, as they allow to capture high-density point clouds of very complex geometries in short time. In addition, the free and usually intricate typology of these parts converts them into evident targets for applying non-contact reverse engineering equipment at the inspection stage. Although the evaluation is only external and performed at the surface level (with the exception of Computerized Tomography), they constitute valid techniques for the dimensional inspection of multiple external geometries, either simple or complex. These optical inspection equipment may become the only suitable techniques due to the high ratio between the number of points captured and the inspection time.

Nevertheless, in order to deploy effectively these techniques, the accuracy that can be reached from the metrological point of view still needs to be determined, beyond the basic application of reverse engineering, i.e., the reconstruction of the geometry [1–5]. Despite the fact that there are already standards [6–9], and specific devices [10–15] designed for assessing optical inspection systems, they are not completely adapted to certain sensors, and the influence of materials, surface finishes, lighting, etc. must be studied [16–20]. The procedures are also diverse depending on the technology used by the

sensor, either laser triangulation in CMM [21–25] or laser triangulation in AACMM [26–28] among other equipment (such as structured light, 2D optical CMM, focus variation, etc.), being adapted to the particularities of each technology and its strategies, technological parameters, etc.

Even choosing a certain non-contact inspection technology, significant advances have been developed in the equipment and sensors themselves. Focusing on the capabilities of the new sensors, the study of the accuracy achievable by these optical equipment is a recurring theme in current research.

With regard to laser triangulation sensors (laser line scanners), it must be said that sensors mounted on coordinate measuring arms (AACMM) are usually much more suitable for reverse engineering tasks, precisely because of their portability and low setup time. On the other hand, CMM-mounted laser line sensors are most used for metrological evaluation of serial parts, due to the better repeatability achieved by machines and software when executing automated inspection programs.

Although it is difficult to compare with each other, as it depends on the machine (AACMM or CMM) and the environmental conditions, it is clear that sensors mounted on CMMs can be more valuable for accuracy purposes, as the sensor is positioned at the optimal focal length and orientated in the normal direction regard the part surface, scanning trajectories are highly repeatable, and the operation is usually performed in a more controlled environment. On the contrary, trajectories are highly dependent on the operator and the strategy in AACMM-mounted laser sensors, generating point clouds with overlapping zones, which lowers the quality of the cloud and increases the influence of the software filter, thus reducing the accuracy of the equipment [29]. In the proposed research, a state-of-the-art laser line scanner mounted on a CMM has been used, so the values obtained with the sensor may be considered as the more accurate that this technology can offer today.

The importance of these systems for the inspection of additively manufactured parts is focusing the research on the development of the most suitable optical systems. Very recent research is showing comparisons of laser triangulation systems with other optical systems, such as Structured Light Scanners or Photogrammetric Scanning Systems [30], or integrating Computerized Tomography (CT) to the comparison [31].

The evolution of laser triangulation sensors has been clear and evident. Apart from the improvement in the quality of certain components (beam stability, laser spot size, miniaturization and weight of the whole, better thermal behavior, duration, etc.), improvements have also been made in the main technological parameters, such as the automatic control of the laser intensity, the camera exposure time, the point densities (both within the laser line and along the scanning direction) or the laser line width, and even the integration of point cloud filters in real time.

These latter aspects have made it possible, for example, that modern laser line sensors are able to capture bright or black surfaces without previous spraying of white developer powder or other coatings over the part surface, which inevitably alter the measurement [32]. The enormous importance of the dimensional precision of the parts should be considered in a process that aims to obtain a functional part. Currently there are already studies and publications about the accuracy of 3D metal laser printing, which are focused mainly on the surface finish [33–35] on the printing limits (avoiding the incorporation of reinforcements or geometrical supports), on the outer but also inner inspection (CT) [36,37], or on the functionality of the printed parts, etc. Less common are the studies that analyze the suitability of the SLM process from the point of view of complying with dimensional and/or geometrical tolerances, analyzing multiple tolerance types (GD&T), and even more, contrasting different optical equipment [38], especially from the micro-geometrical point of view.

Unfortunately, the surface of the parts printed by SLM shows very particular trajectory patterns, [39–43], generating drops on the surface, grooves (similar to welding beads) and a very high roughness which depends on many factors, such as the laser beam speed, power, material grain size, alloy composition, strategy, etc. All these factors increase the difficulty in obtaining scans with high accuracy, compelling to control of these parameters by current and future AM equipment [44].

Post-processes such as sandblasting are often used to improve the surface finish of unique parts manufactured by SLM whereas more automated processes such as electropolishing are reserved for serial or very complex parts [45]. These operations for improving the surface finish are imperative in many applications (dental implants, prostheses, etc.). Therefore, it is essential to know the limits of dimensional and geometric accuracy achievable in optical scanning of these very particular surfaces. Furthermore, the sandblasting post-process favours the inspection of parts with optical systems. In [46] it was found that the best correlation between contact and non-contact measurements was obtained in surfaces with a random pattern formed by not very deep craters, similar to the finish of EDM (Electrical Discharge Machining) and Shot-blasting (Shot-blasting with spherical grain), due to the absence of shiny or reflective surfaces.

This work proposes to perform a metrological evaluation (GD&T type) of a laser sensor mounted in CMM, verifying its suitability to evaluate the SLM process. In addition, a complete study is also included about the types of filters incorporated by different software used in reverse engineering processes. These filters are applied to improve the quality of the point clouds, eliminating spurious points and reducing the weight of files. As conclusions, the limits of accuracy attainable with the laser sensor and the selection of the most suitable filters will be obtained. Moreover, the dimensional accuracy with which the SLM machine is capable of manufacturing a test part will also be obtained indirectly. The contact measurement of the metal-printed part, before and after sandblasting, will allow to analyze the influence of the sandblasting post-processing.

The following sections describe the available equipment together with the proposed methodology, experimentation and obtained results. Section 2 is dedicated to explain the methodology followed in this work. In section 3, the design of the test artifact is discussed, as well as the details of its manufacture (materials and equipment). Section 4 details the process of part measurement by contact, both in as-built and post-sandblasting conditions and its results. In section 5, the measurements performed with CMM-mounted laser line sensor are described. Finally, in section 6, different methods implemented in different software applications for filtering point clouds are studied aiming at improving the measurement quality.

2. Methodology

The proposed research starts from results of previous studies [47] within a project aimed at the metrological evaluation of the SLM process. That project was focused on determining the dimensional errors caused by defects in positioning and dosing of the roller in the parallel (roller axis) and perpendicular directions (roller feed direction). For this purpose, a test artifact consisting of a matrix of cubes with faces oriented parallel to the Cartesian axes of the printer was manufactured and evaluated. Thus, the errors committed in the feed direction were clearly differentiated from those in the roller axis direction, and from those in the built direction (height). This research already pointed towards the design of a more generic artifact, consisting of non-flat surfaces whose manufacture involves a much larger machine working volume. At the same time, these surfaces should have a complete metrological definition, in order to guarantee the traceability in the evaluation regarding the manufacturing and inspection accuracy.

To perform the metrological verification, a test artifact is designed and developed ad-hoc, taking into consideration both the manufacturing process and the metrological and reverse engineering equipment available. A part consisting of multiple spheres has been designed, as the sphere is a feature whose metrological inspection allows to ensure the traceability of comparisons. This test artifact was manufactured in 17-4 PH stainless steel using the optimal parameters previously determined for the available SLM machine [48].

As shown in Fig. 1, the methodology followed in this research was as follows:

1- A test artifact is designed adapting its size to the working volume of the metal printer. The artifact consists of a set of spheres, features with a complete geometric and metrological definition which simplifies the measurement both by contact and by the laser line sensor, mounted in the same CMM.

2- 3D printing of the test artifact. Once the CAD design has been exported to STL format, the part is printed in 17-4PH on the SLM machine. The optimal process parameters previously set are used for this purpose.

3- Measurement of the part using contact probing in the CMM. It is first measured in the "as built" state. Data obtained from the CMM measurement are compared with data from the original CAD, providing information about the accuracy achievable by the SLM printer.

4- Sandblasting of the part with fine sand (alumina powder).

5- Measurement of the sandblasted part in the CMM. Multiple repetitions (10) are carried out in order to apply error correction techniques thus providing with reliable reference data. The comparison between “post-sandblasting” and “as built” measurement data will permit to know the effect caused by sandblasting on this kind of geometries.

6- Measurement of the sandblasted part with a laser line sensor (in CMM). In this stage, a previous study is carried out about the most suitable scanning strategy aimed at generating high quality point clouds.

7- Analysis of the point clouds obtained with the laser sensor. This analysis involves extracting different types of dimensional and geometric measurements (GD&T) from the point clouds. In this stage, different types of filters provided by different reverse engineering software, such as PC-DMIS (laser scanner control), Geomagic Control, PolyWorks, 3DReshaper or GOM Inspect, will be evaluated.

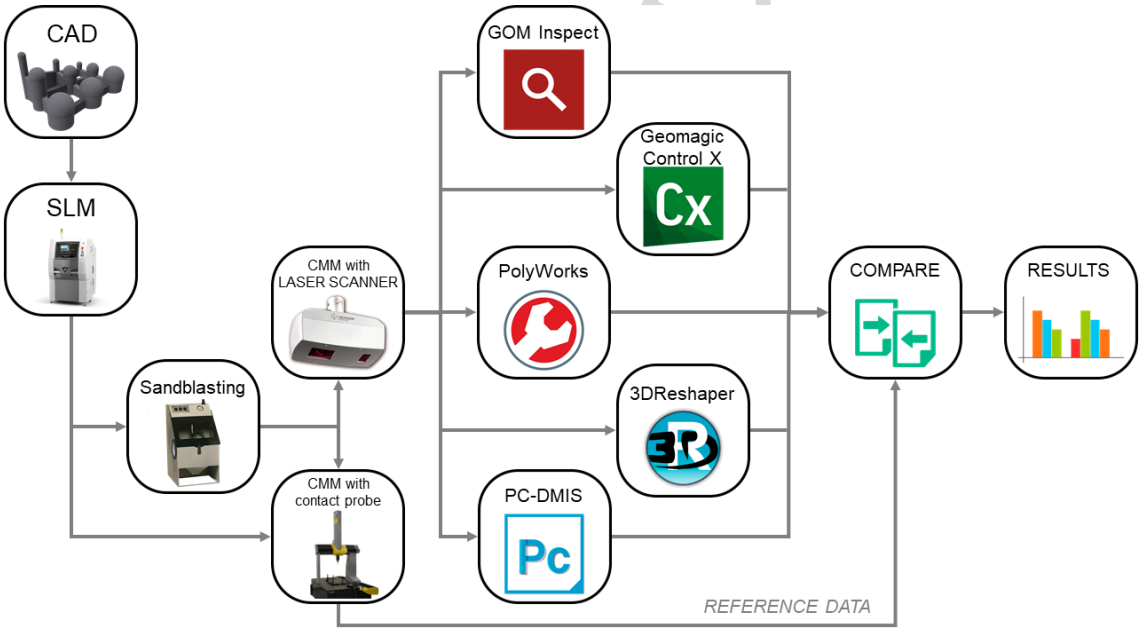

Fig. 1. Research methodology

In the following sections, each of these steps will be explained, as well as the equipment and materials used, and the results obtained.

3. Design, printing, and post-processing of the test artifact

In the design of the test artifact, the manufacturing process, and the capacity of the available SLM machine have been taken into account. A 3DSystems SLM ProX DMP 100® printer has been used. It uses a fibre laser of 50 W max. and 1070 nm of wavelength (Nd-YAG), in a controlled atmosphere (Nitrogen) at 7 bar approx. For printing this artifact, the power was set at 38 W with a deposition layer thickness of 30 µm. It should be noted that the maximum printable volume available is 100x100x100 mm with a repeatability of 20 µm in the 3 axes and accuracy of ±0.1-0.2% with a ±50 µm minimum.

The material chosen for the manufacture of the test part is 17-4PH stainless steel, supplied by 3DSystems. This is an alloy of Cr (15-17.5%), Ni (3-5%) and Cu (3-5%) among other components in lower percentages (Nb, Si, Mn). It is a very common material in industries such as aerospace, chemical processes, food and mechanical components in general, especially because of its high mechanical strength (similar to AISI 304), its good corrosion behaviour, and the possibility of improving its mechanical properties by means of heat treatment (ranging from a nominal yield strength of 620 MPa in its "as-built" condition, to 1100 MPa after an appropriate heat treatment, as well as variation of hardness from 300 HV5 to 400 HV5 with a suitable heat treatment).

Taking into account the manufacturing requirements of our machine, the test artifact has been designed by including a set of spheres of different diameters distributed on the printing baseplate (Fig. 2). This type of entity has been chosen as it is an entity type perfectly defined mathematically and metrologically. There are well-established algorithms for their measurement by contact with maximum accuracy, providing values of the diameter, center location and form error of each sphere, as well as of the distances between them. In fact, the artifact emulates those used in the verification and certification of CMMs (ISO 10360). As it is indicated in that standard, the distances between spheres centres are measured when the artifact is located in different positions and orientations within the CMM volume (e.g., along the X, Y, Z axes, or along the diagonals of the XY, XZ, YZ planes or along the XYZ cubic diagonal). Likewise, the size and distribution of the spheres allows them to be measured by both inspection systems used (contact and optical).

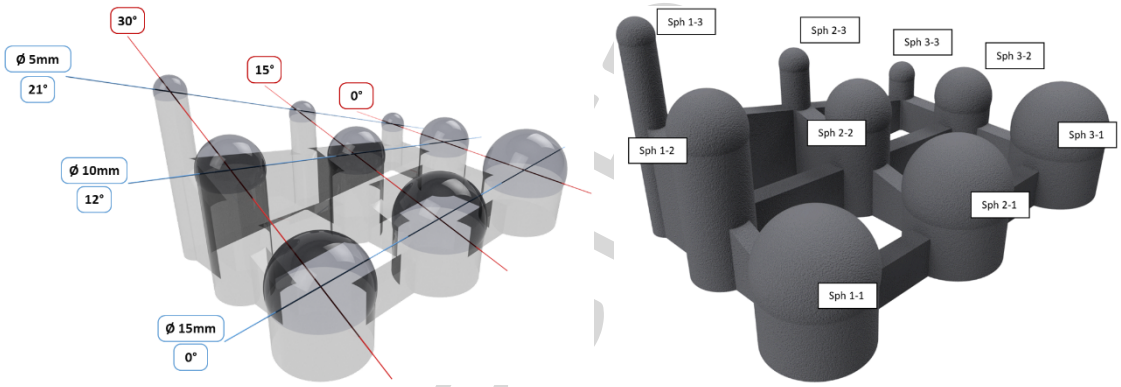

(a) (b)

Fig. 2. 3D CAD model of the new test artifact for the evaluation of the SLM process: (a) design characteristics and (b) nomenclature of the spheres.

The spheres are supported by cylindrical pillars of smaller diameter in order to hold them without the need to print a support structure. The cylindrical pillars have been joined by vertical walls to maintain invariable the distances between spheres during the operation that involves the separation of the artifact from the machine baseplate after printing. These walls are thick enough to be able to separate the part from the baseplate, allowing this cutting operation by any external manufacturer. This will make it possible to contrast between different types of SLM printers in the future.

As shown in Fig. 2, the design of the test part includes 9 spheres, 3 spheres of 5 mm diameter, 3 of 10 mm diameter, and 3 of 15 mm diameter. The spheres were encoded by rows and columns (Fig. 2(b)) so that Sph 1.1, Sph 2.1 and Sph 3.1 are the 5 mm diameter spheres, Sph 1.2, Sph 2.2 and Sph 3.2 are the 10 mm diameter spheres, and the Sph 1.3, Sph 2.3 and Sph 3.3 are the 15 mm diameter spheres. The centres of the spheres have been placed forming a range of 3 different inclinations (Fig. 2(a)), with angles of 0°, 10° and 30° parallel to the baseplate, respectively. In this way, the height of the spheres reaches values representative of the SLM printer working volume (printing at heights above 55 mm of a maximum total of 80 mm, which is a considerable height for that volume).

In the first phase of the experiment, the part is measured under "as built" conditions. The reference values are obtained along with the deviations between the SLM printed artifact and the CAD model. Subsequently, the part is sandblasted in order to improve, on the one hand, its surface finish, and on the other, its suitability for measurement by optical equipment.

A Sablex S-2 sandblasting machine with a working pressure of 7 bar and an incidence area of 4 mm in diameter has been used for the sandblasting process. White aluminium oxide (WFA) powder with particle size F100 (FEPA 100mm diameter) has been used as sand. During sandblasting, an incidence distance of about 30 mm was maintained for 3-4 seconds in several different orientations. It is a manual process performed with multiples orientations, that is, from the 4 cardinal points with some elevation and a perpendicular direction.

4. Contact measurements (CMM): "as-built" and "post-sandblasting" stages

The proposed evaluation method includes contact probing of multiple points in a CMM. For this task, a CMM DEA Global Image 91508 (Hexagon Metrology) was used. This machine is equipped with a Renishaw PH10MQ indexed head. This head allows to incorporate different types of sensors, in particular, touch trigger probes (point-to-point), continuous contact probes (scanning) and laser triangulation sensors. In this research, a Renishaw SP25® touch scanning probe with a stylus of 1 mm diameter ruby tip was used for the measurement of the test artifact by contact. The Maximum Permissible Error is MPE_E [µm] = 2.2 + 0.003 · *L* [*L* in mm] (according to ISO 10360-2). In addition, several techniques were applied to compensate the usual errors in CMM measurement, such as multi-position measurements with mutual measurement method and repetitions.

Fig. 3 shows the CMM measurement process for the as-built part (Fig. 3 (a)) and for the after-sandblasting part (Fig. 3 (b)). In both cases, the strategy involved probing a high-density uniform distribution of points, located on and above the sphere equator (Fig. 3 (c)). The number and distribution of points was established as a function of the sphere diameter, so that the density of the scans for all the measured spheres was roughly equal (approximately 2.55 points/mm^2). In particular, 900 points were probed in the 15 mm diameter spheres (distributed in 19 rows or heights along the top hemisphere), 400 points in the 10 mm diameter spheres (13 rows) and 100 points in the 5 mm diameter spheres (9 rows).

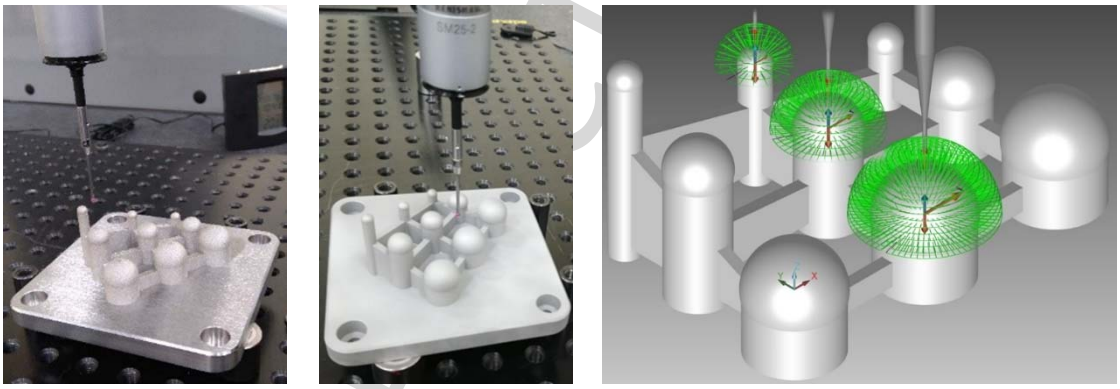

(a) (b) (c)

Fig. 3. Contact measurement of the test artifact: (a) in as-built condition and (b) after-sandblasting condition. (c) Distribution of points for the ∅15mm, ∅10mm y ∅5mm spheres (same density).

Different GD&T measurements and deviations were evaluated. Regarding dimensional deviations, sphere diameters and distances between centers were calculated, considering only the distances between spheres of same diameter in this last case. Regarding geometric deviations, the form error of the spheres and their centre location were considered. With these reference dimensions measured by contact, a "quasi-real" CAD model was generated by assigning the actual value of the diameter and spatial location of the spheres. This quasi-real CAD model will be used as reference for comparing with the results obtained with the laser line sensor (CMM laser).

Table 1 shows some of the measurement results, for the as-built part condition (before sandblasting) and for the after-sandblasting condition. The values represent the difference between the nominal CAD and the SLM test artifact measured by the CMM (dimensional and geometrical deviations)

Table 1. GD&T deviations in the nine spheres for the as-built and post-sandblasting conditions

GD&T evaluation		As-built		Post-sandblasting		Blasting Erosion ratio	Improvement form error ratio
		Average [mm]	Standard deviation [mm]	Average [mm]	Standard deviation [mm]	[mm]	[mm]
Dimensional (Diameters)	Ø5	-0.1038	0.0078	-0.1563	0.0096	0.0525	
	Ø10	-0.1234	0.0091	-0.1706	0.0064	0.0472	
	Ø15	-0.1356	0.0156	-0.1861	0.0071	0.0505	
Geometrical (Form error)	Ø5	0.1032	0.0163	0.0957	0.0239		0.0075 (7.83%)
	Ø10	0.0936	0.0152	0.0836	0.0191		0.0100 (12.01%)
	Ø15	0.1001	0.0070	0.0783	0.0014		0.0218 (27.86%)
Dimensional (Center Position)	Dx	-0.0243	0.0217	-0.0273	0.0217		
	Dy	-0.0129	0.0148	-0.0084	0.0135		
	Dz	-0.0088	0.0238	0.0033	0.0215		

As shown in Table 1, the diameters of spheres in the as-built part are smaller than the nominal CAD values. Values of deviations range between -0.1038 mm (Ø5 mm sphere) and -0.1356 mm (Ø15 mm sphere). Standard deviation values (σ) of diameter deviations are comprised between 0.0078 and 0.0091 mm, with 10 measurement repetitions, for the Ø5 mm sphere and Ø10 mm sphere, respectively. For the biggest Ø15 mm spheres the standard deviation rises to 0.0156 mm.

After sandblasting, the measurements indicate that all the spheres have a diameter far smaller than the as-built value. The diameter deviations are -0.1563 mm (Ø5 mm spheres), -0.1706 mm (Ø10 mm spheres) and -0.1861 mm (Ø15 mm spheres) (Table 1).

It is interesting to note that, during the finishing of parts manufactured by SLM, sandblasting causes a very constant erosion rates, about 0.05 mm as average for all the spheres. This is due, on the one hand, to the erosion effect caused by sandblasting and, on the other hand, to the flattening effect of crests and peaks (caused by projections, prominent and solidified hemispherical drops, etc.). The fact that the erosion rate is constant and independent of diameter and position of the spheres on the plate, suggests that a manual sandblasting can be sufficiently uniform and homogeneous on all surfaces. This is something that was not predictable a priori, but whose verification validates in some way the sandblasting as a homogenizing process of the surface. Once the influence of erosion rate is known, the nominal CAD design can be corrected to obtain manufactured spheres with more accurate diameters.

From the point of view of the spheres form error, the SLM 3D printer manufactures the test part with an error of the order of 0.1 mm (as-built condition). This value is almost independent of the sphere size, Ø 5 mm (0.1032 mm), Ø 10 mm (0.0936 mm) or Ø 15 mm (0.1001 mm). However, the sandblasting process greatly affects the form error depending on the diameter of the sphere. For the Ø5 mm spheres, the improvement in the form error is only 0.0075 mm (from 0.1032 to 0.0957 mm), a 7.83% of improvement. For Ø10 mm spheres, the form error is reduced from 0.0936 to 0.0836 mm, an improvement of 12.01%. Finally, for the Ø15 mm spheres, the form error decreases from 0.1001 to 0.0783 mm, an improvement of 27.86%. That means that, as far as the diameter increases, the area exposed to the sandblasting is greater and the improvement in the form error is higher.

5. Scanning with CMM and laser line sensor

The test artifact in the condition after-sandblasting was measured with a laser line sensor mounted on the CMM. The laser scanner converts the CMM into a multisensor system, combining traditional touch probing with optical measurements. This capacity enables to use both systems to capture surface geometry or feature measurement using the same CMM program. The laser sensor is the state-of-the-art HP-L-10.6 model from Hexagon Metrology. Table 2 shows the main technological parameters. The sensor uses the "Flying-Dot Technology", whereby the light intensity is automatically adjusted point by point (10 times/point) providing an excellent optical dynamic range. This means that this laser scanner is less sensitive to ambient light and surface changes, therefore generating point-clouds of high quality and

reliability. In addition, the line width can be selected to be 24 mm, 60 mm to 123 mm, as required. The point-to-point distance varies depending on the chosen line width. Regarding the capture density, it allows densities from 8.4, 16.8 to 33.5 points/mm, achieving very high capture speed up to 30,000 points/s.

Table 2. Main technological parameters of the HP-L-10.6 Laser Scanning Sensor

Feature	**Value**
Laser protection class	2 (IEC 60825-1: 2007)
Laser wavelength	690 nm (Visibly red)
Standoff and depth (Z)	170 +/- 30 mm
Line width	3 options: 24, 60, 123 mm
Points density	3 options: 8.4, 16.8, 33.5 pts/mm
Measuring accuracy ISO 10360-8:2013*	Probe dispersion value ($P_{Form.Sph.D95\%:,MPL}$): 34 µm Probing form error ($P_{Form.Sph.1x25:,MPE}$): 22 µm
Maximum lines per second	53 Hz
Maximum data rate	30,000 pts/s
Sensor Size L x W x H	134 x 72 x 60 mm
Weight	360 g
Power Supply	DC 18 to 28 V, 170 to 200 mA, protected against polarity reversal

*Values are including expanded measurement uncertainty according ISO 17865:2016. Measured using a manufacturer supplied sphere and plane artefact, each certified by an independent accredited lab.

The software PCDMIS 2018 R2 which controls the CMM was used initially to digitize the test part. This software allows to control the laser sensor and to capture the point-cloud. Also, it offers different filters. A density of 16.8 points/mm and a laser line width of 123 mm were selected for the acquisition, so that the points could be captured with the same orientation in all the spheres (top hemisphere). However, several CMM head orientations were necessary to achieve sufficient coverage of the top hemisphere. In particular, five scanning passes capturing points in all the nine spheres were carried out: 1 pass with vertical orientation (A0B0 orientation of the indexable probe PH10-MQ, Fig. 4 (a)) and 4 passes with elevation of 45° according to the cardinal orientations/directions, as it is shown in Fig. 4 (b,c,d,e). This way points located slightly below the equator are also captured, which increases the accuracy in the measurement of diameter and center coordinates of all the spheres.

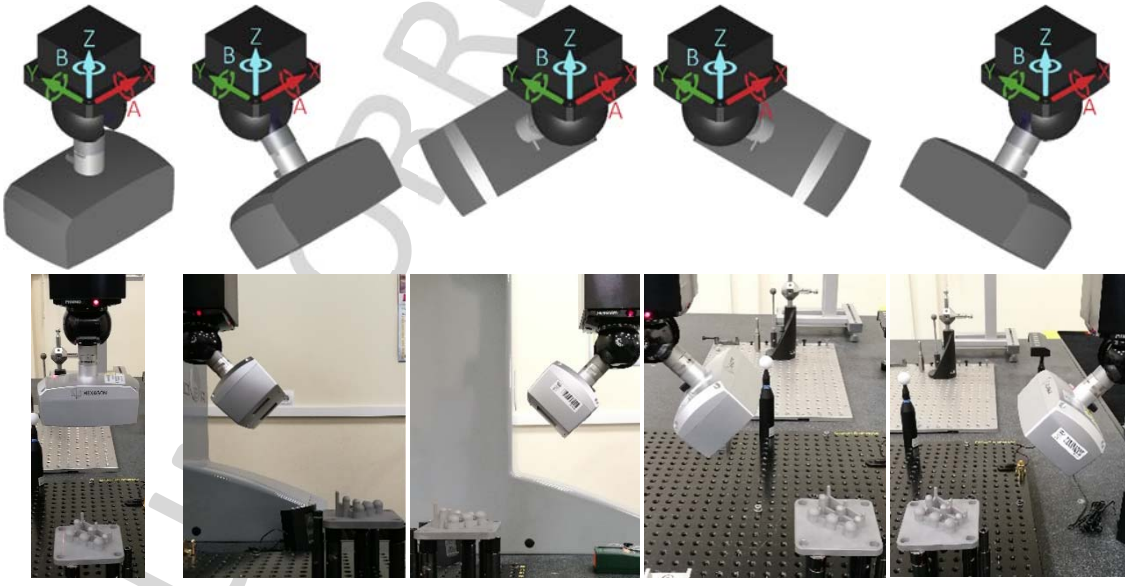

(a) (b) (c) (d) (e)

Fig. 4. Laser scanning sensor orientations used: (a) A0B0, (b) A45B0, (c) A45B180, (d) A45B90 and (e) A45B-90.

During the scanning of the test artifact a pre-filter was used which limits the digitizing to those regions that have an optimal orientation with respect to the sensor. This filter constraints the capture of points

to those that are close to the normal between laser and part surface, choosing a limit value of 75°. This implies that only high-quality points are acquired. The complete coverage of the spheres for their successful reconstruction was guaranteed with the 5 scanning passes, around 5,000 points/sphere for the Ø5 mm spheres, 20,000 points/sphere for the Ø10 mm spheres and 45,000 points/sphere for the Ø15 mm spheres.

As a side effect, points belonging to the side walls and cylindrical pillars which support the spheres were also captured (Fig. 5 (a)). Consequently, it was necessary to carry out operations for cleaning and trimming the point-clouds aiming at keeping only the points that belong to the spheres (Fig. 5 (b)). Once cleaned and trimmed, the point-clouds were exported to be processed by different reverse engineering and metrology software, following the methodology shown in Fig. 1. The process involves reconstructing the spheres from the point-clouds, and then evaluate the diameter, the center location, the form error and the value of standard deviation of each sphere. Additionally, an alignment is performed using the 3-2-1 method as shown in Fig.5 (b,c), that is, centers of spheres 1.1 (dark blue), 3.1 (yellow) and 3.3 (orange) were used to level the XY plane; centers of spheres 1.1 (dark blue) and 1.3 (yellow) to define the X axis; and the center of the sphere 1.1 to locate the origin. Later, the point-clouds of the nine spheres will be used to obtain a global 3D comparison between the scanned spheres and the "quasi-real" CAD model (Fig.5 (c)).

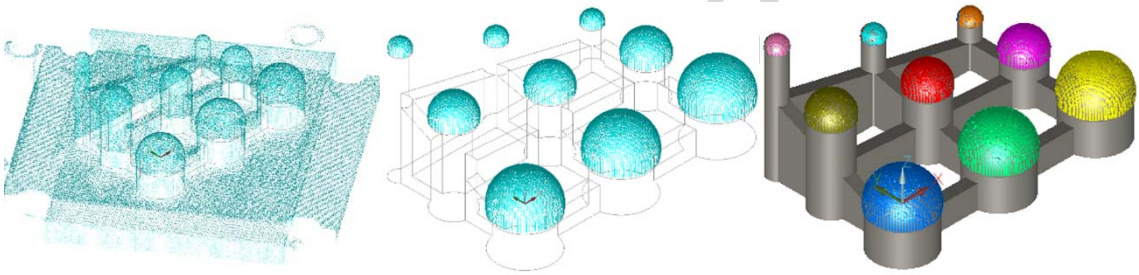

(a) (b) (c)

Fig. 5. (a) Raw point-cloud. (b) Cleaned and trimmed point-cloud. (c) 3D CAD comparison between the processed point-cloud and the quasi-real CAD model.

Fig. 6 shows the measurements regarding the diameter deviation and form error of the best-fit spheres reconstructed from the point-clouds. These results were obtained using PC-DMIS software, but other software applications were also used for validating the results, leading to the same values when analyzing cleaned point clouds without any filtering.

Deviations in sphere diameters captured by the laser and the reference values obtained with the CMM are in the order of 0.1 mm of average value (Fig. 6 (a)) for all the spheres. In all cases, laser measured diameters are smaller than the values measured by the CMM (green-discontinuous curve).

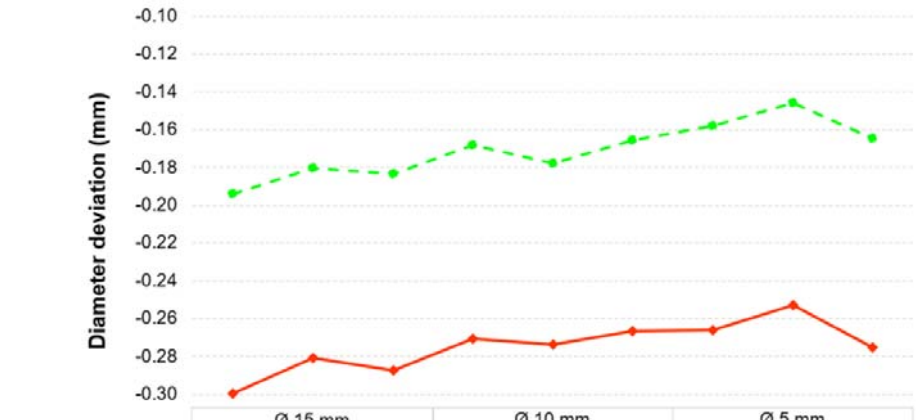

	Ø 15 mm			Ø 10 mm			Ø 5 mm		
	SPH 1.1	SPH 2.1	SPH 3.1	SPH 1.2	SPH 2.2	SPH 3.2	SPH 1.3	SPH 2.3	SPH 3.3
Laser Scanning	-0.2996	-0.2806	-0.2876	-0.2709	-0.2735	-0.2666	-0.2660	-0.2529	-0.2752
CMM	-0.1942	-0.1806	-0.1836	-0.1684	-0.1778	-0.1657	-0.1582	-0.1459	-0.1649

(a)

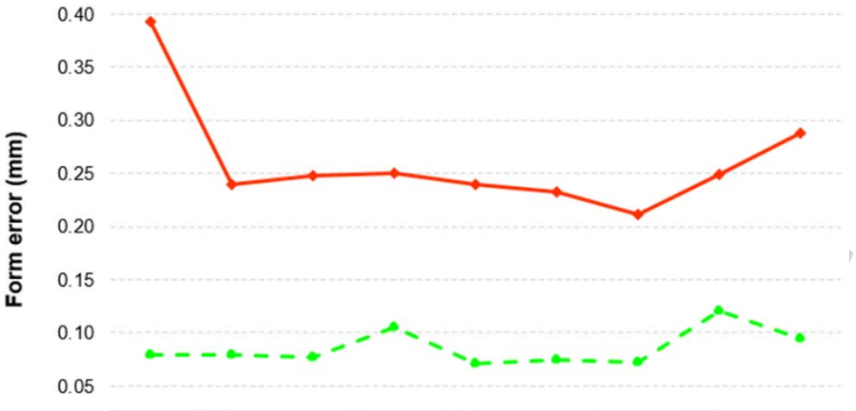

	Ø 15 mm			Ø 10 mm			Ø 5 mm		
	SPH 1.1	SPH 2.1	SPH 3.1	SPH 1.2	SPH 2.2	SPH 3.2	SPH 1.3	SPH 2.3	SPH 3.3
CMM	0.0789	0.0794	0.0767	0.1056	0.0711	0.0741	0.0726	0.1204	0.0941
Laser Scanning	0.3929	0.2401	0.2475	0.2508	0.2398	0.2329	0.2115	0.2485	0.2881

(b)

Fig. 6. Comparison of sphere measurements obtained by contact (CMM) and without contact (Laser Scanning): (a) deviation of diameter from the CAD nominal geometry, (b) form error.

Concerning the form error (Fig. 6 (b)), although the measured deviations are already high for the contact measurement, deviations of form error for laser measurements are even higher, with an average around 0.2 mm further from the real value. This deviation is even higher in some cases with values of 0.3 mm (Sphere 1.1 - ∅15 mm).

The definition of the form error described in the ISO 1101:2017 standard [49] is not adequate to measure the quality of the point cloud, from a metrological point of view. The reason is that if a single point or some few points are located very far from the diameter of the best fit sphere (obtained by least squares sphere fit), the error value will be excessive and unrealistic. These are the so-called spurious points, which usually appear above the scanned surface (several tenths of millimeter and even millimeters), but sometimes they can be located inside the part.

As aforementioned, the surface finish of parts manufactured by SLM shows significant irregularities. Although this effect is minimized to a great extent with the subsequent sandblasting process, the surface still has zones with variable brightness which causes measurement errors when optical methods are employed. In Fig. 7, a microscopic image shows the irregularities in different areas of the surface for one of the spheres after the sandblasting process.

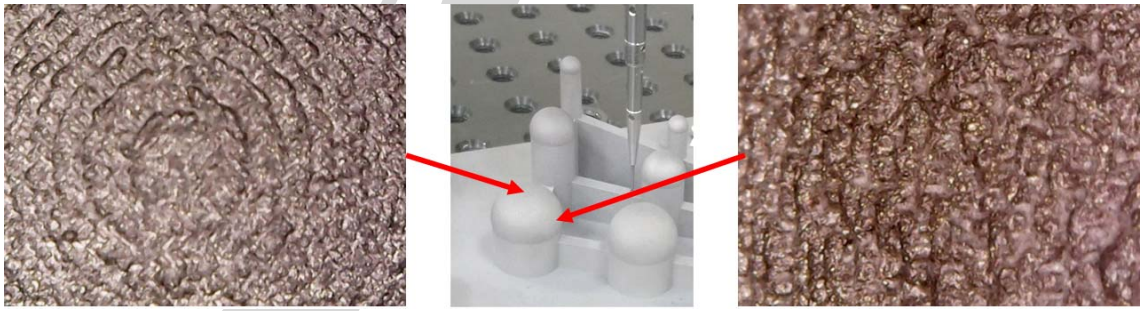

Fig. 7. Microscope images (100x) of a SLM manufactured sphere after sandblasting: (left) sphere top, (right) sphere side.

In view of the results, this research proposes to study the point-cloud quality (laser) based on another parameter usually available in metrological and reverse engineering software. This involves considering the standard deviation (σ) of the best-fit sphere to the point cloud. Fig. 8 shows the meaning of this concept applied to the sphere diameter. It can be observed how this value allows a much better measurement of the point-cloud quality corresponding to a scan on a section. Taking into account that

the spheres are best-fitted from point-clouds of about 45,000, 20,000 and 5,000 points, for Ø15, Ø10 and Ø5 mm spheres, respectively, it makes sense to apply a filter to consider only the inner points of 1σ, 2σ, 3σ, or even 6σ if a high-density point-cloud is desired. The objective of this filter is to eliminate spurious points (Fig. 8 (a)), which appear usually on the horizon (boundary) of the visualization for a given sensor orientation. On the contrary, the loss of accuracy in the diameter value is minimal.

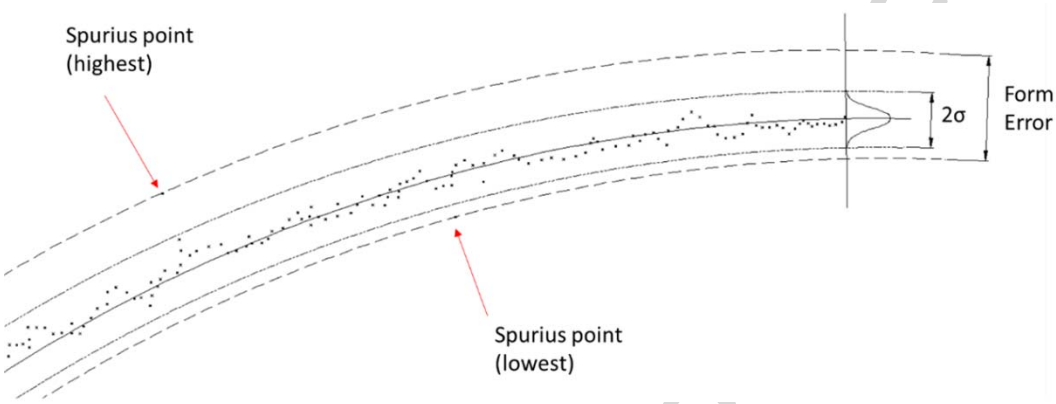

(a)

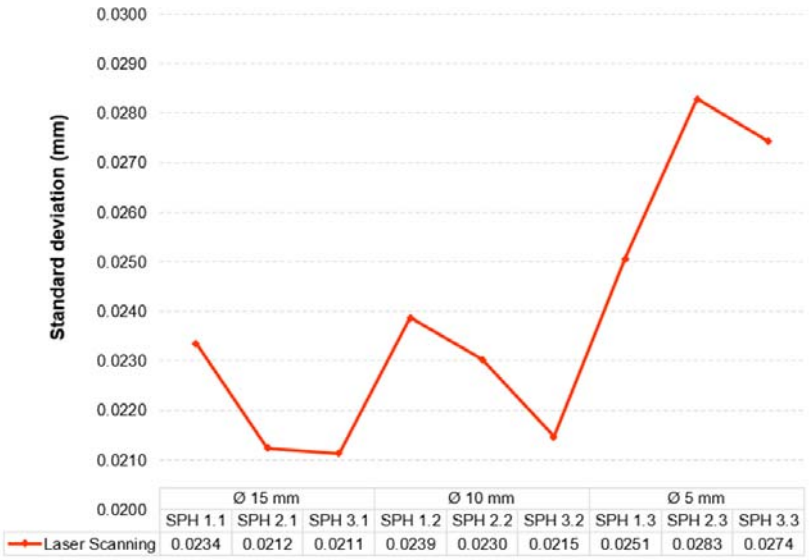

	Ø 15 mm			Ø 10 mm			Ø 5 mm		
	SPH 1.1	SPH 2.1	SPH 3.1	SPH 1.2	SPH 2.2	SPH 3.2	SPH 1.3	SPH 2.3	SPH 3.3
Laser Scanning	0.0234	0.0212	0.0211	0.0239	0.0230	0.0215	0.0251	0.0283	0.0274

(b)

Fig. 8. (a) Meaning of the point-cloud standard deviation parameter. (b) Value of the standard deviation of the raw point-cloud (without filtering).

6. Application of filters to the point clouds

First, it is necessary to define the meaning of improving the quality of the point-cloud. In this sense, filters can be applied to improve the two parameters that best define the spheres: diameter (obtained by least squares fit) and form error. The value of these parameters as measured by contact probing in the CMM will be taken as the limit for the improving of the applied filter.

Five different software applications were used for treating the point-clouds obtained by the laser line sensor: PC-DMIS® (CMM with touch probe and laser sensor), Geomagic Control X®, 3D Reshaper®, Polyworks®, and GOM Inspect®. All these top level packages have specific modules for point-cloud management, mesh creation and surface analysis. They include color map representation of deviations, feature extraction and advanced functions for treating, filtering, and measuring point-clouds. These last functionalities are especially interesting for the present work.

Fig. 9 shows screenshots of the mentioned software after generating the spheres from the same point cloud previously illustrated in Fig. 5 (b) by applying the same best fit algorithm based on least squares.

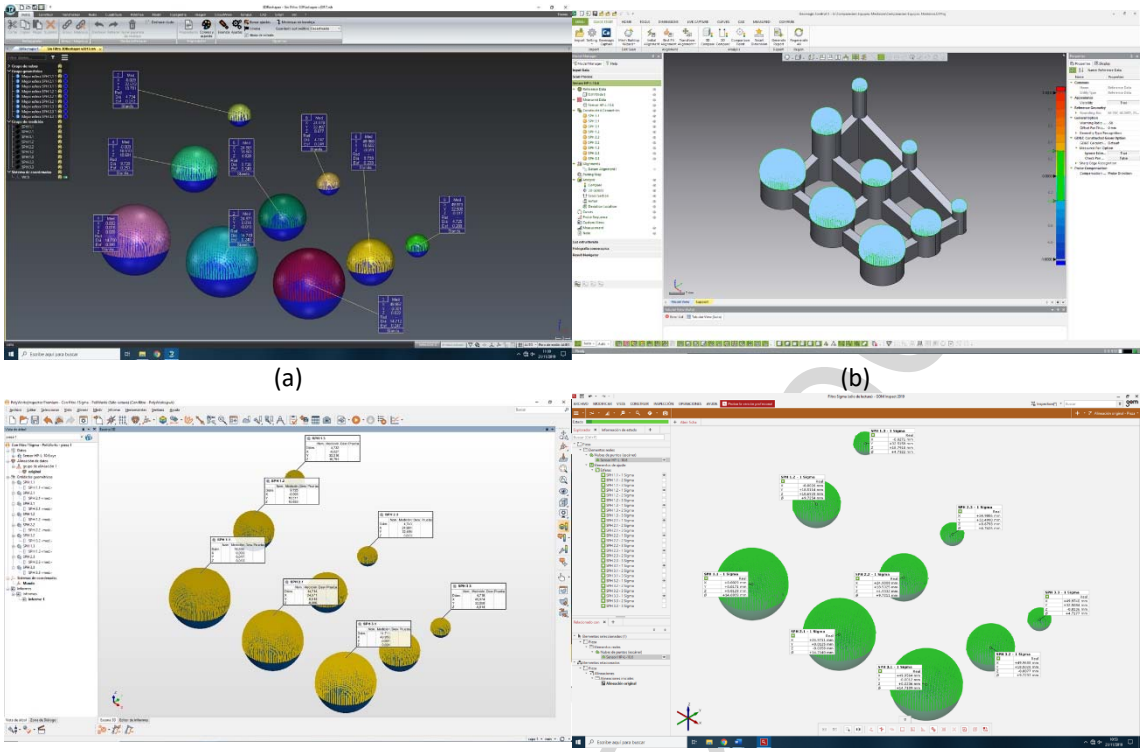

(a) (b)

(c) (d)

Fig. 9. Screenshots of the software used to generate best fit spheres: (a) 3D Reshaper, (b) Geomagic Control X, (c) Polyworks and (d) GOM Inspect.

Nevertheless, one of the main problems found in this research was that each software implements its own set of filters. However, all the studied software packages share a common element: filters that remove spurious points, those which are located furthest away from the average value.

The way to eliminate these points is somewhat different depending on the considered software, but in general these filters are closely related to the standard deviation. Obviously, as the spurious points are removed, the sphere parameters (diameter and form error) converge towards values that can be either closer or farther to the corresponding parameters in the quasi-real CAD model. Fig. 10 shows the evolution of sphere parameters, firstly without filtering (directly with the clean point cloud obtained from the laser sensor), then filtering the points located far away from 3σ, 2σ or 1σ, respectively (σ is the value of the standard deviation of the best fit sphere). The software used in this example was Polyworks.

In the case of the diameter (Fig. 10 (a)), when applying the filter, the value is farther away from the reference value obtained by contact. This difference is even greater if more restrictive filters 2σ or even 1σ are applied. However, despite the values obtained for the diameter, this difference is insignificant, about 1 or 2 µm. In any case, an important difference is observed between results from contact probing and from laser sensor, which always provides diameters about 0.1 mm smaller. This difference is undoubtedly due to the type of surface generated by the SLM process.

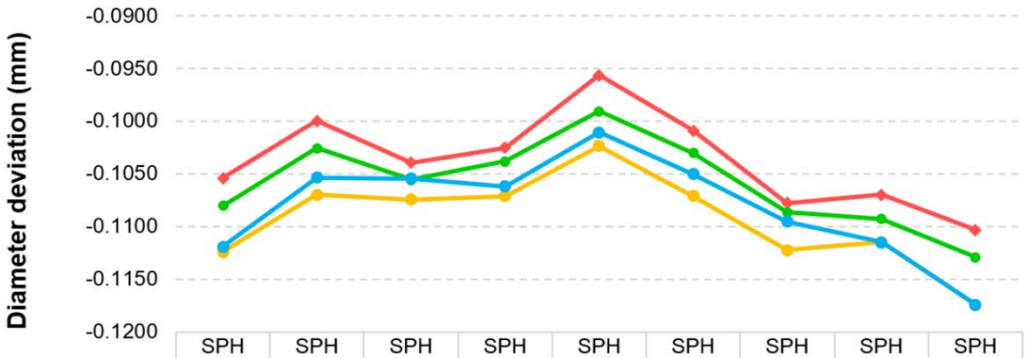

	SPH 1.1	SPH 2.1	SPH 3.1	SPH 1.2	SPH 2.2	SPH 3.2	SPH 1.3	SPH 2.3	SPH 3.3
Laser Scanning	-0.1054	-0.1000	-0.1040	-0.1025	-0.0957	-0.1009	-0.1078	-0.1070	-0.1104
3*Sigma Filter	-0.1080	-0.1026	-0.1056	-0.1038	-0.0991	-0.1030	-0.1087	-0.1093	-0.1130
2*Sigma Filter	-0.1124	-0.1070	-0.1075	-0.1071	-0.1024	-0.1071	-0.1123	-0.1115	-0.1175
1*Sigma Filter	-0.1119	-0.1054	-0.1055	-0.1062	-0.1011	-0.1050	-0.1096	-0.1115	-0.1175

(a)

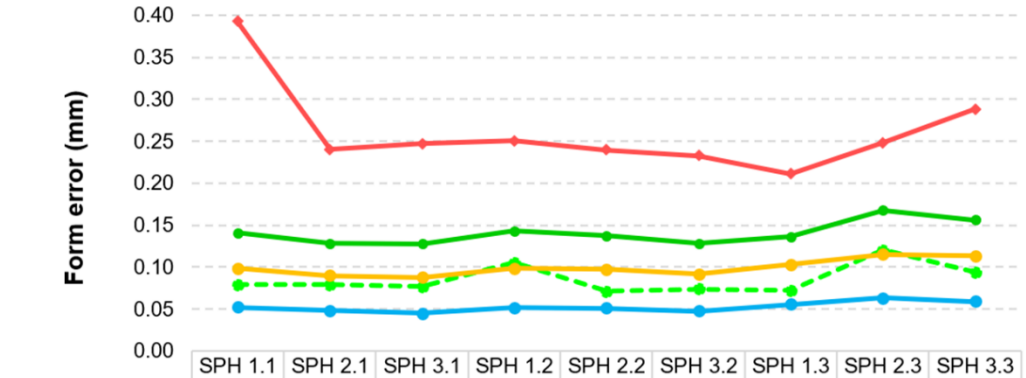

	SPH 1.1	SPH 2.1	SPH 3.1	SPH 1.2	SPH 2.2	SPH 3.2	SPH 1.3	SPH 2.3	SPH 3.3
CMM	0.0789	0.0794	0.0767	0.1056	0.0711	0.0741	0.0726	0.1204	0.0941
Laser Scanning	0.3929	0.2401	0.2475	0.2508	0.2398	0.2329	0.2115	0.2485	0.2881
3*Sigma Filter	0.1406	0.1280	0.1279	0.1429	0.1375	0.1282	0.1363	0.1680	0.1562
2*Sigma Filter	0.0982	0.0899	0.0880	0.0984	0.0975	0.0913	0.1028	0.1155	0.1137
1*Sigma Filter	0.0523	0.0481	0.0449	0.0514	0.0511	0.0477	0.0556	0.0632	0.0591

(b)

Fig. 10. Results of applying different standard deviation filters: (a) deviation of diameter values with respect to the quasi real CAD model (CMM contact values); (b) form error.

In the case of the form error (Fig. 10 (b)) of the SLM manufactured and sandblasted spheres, the application of this type of filters is much more significant. In fact, a great advantage is observed when applying the filters to a point-cloud captured by a laser sensor, especially for a SLM manufactured surface. Whereas the reference values (measured by contact) for the spheres range between 0.0711 and 0.1204 mm, the form error of the spheres reconstructed from the unfiltered point clouds (measured by laser) is about 0.25 mm. When applying a relatively smooth filter that eliminates only the points far away than 3σ, the form error falls below 0.16 mm (Fig. 10 (b)). If a more restrictive 2σ filter is applied, the value is roughly equal to the one obtained by contact. On the contrary, applying the most restrictive filter of 1σ, a false (unrealistic) value is obtained for the form error, in the order of 0.05 mm.

Summarizing, the application of 2σ filter (yellow curve) provides the best fit of the laser point-cloud to the contact point-cloud. The 3σ filter (green curve) is also valid, even more conservative from the point of view that it never provides values lower than the reference ones, measured by contact.

For the previous study, the N*Sigma filter available in Polyworks software was applied. This filter is based on using the standard deviation of the point-cloud. The N*Sigma method requires a N value and excludes data that is larger than N times the standard deviation, also known as the Sigma. This type of filter is also available in GOM Inspect and Geomagic Control software with very similar results. However, in the case of the 3DReshaper software only a percentage-based filter is available. This filter removes the points

furthest from the constructed sphere in the given percentage. In the case of Polyworks and Geomagic Control software, they also have the possibility of applying this percentage filter. Geomagic Control also includes the option of applying a distance filter which eliminates the points located at a higher distance from the radius of the primitive reconstructed sphere.

Table 3 (left) shows the percentage of points eliminated for each sphere when applying the mentioned 3σ, 2σ and 1σ filters in the case of Polyworks software. The behavior is similar for the other software analyzed. From the results obtained with each filter for each sphere, the value of the distance from which points are being removed can be obtained. This provides the value for the distance filter that produces the same filtering effect, that is, that removes the same percentage of points, but without affecting the measured diameter and center location.

Table 3. Percentage of points removed based on the applied filter (filter N*Sigma) and equivalent distance (with respect to the best-fit sphere boundary manufactured by SLM) from which the points are removed.

	Percentage of removed points [%]			**Distance from which points are removed [mm]**		
Spheres	**1σ filter**	**2σ filter**	**3σ filter**	**1σ filter**	**2σ filter**	**3σ filter**
SPH 1.1 (Ø5)	30.76	3.74	0.54	0.0234	0.0467	0.0701
SPH 2.1 (Ø5)	31.52	3.85	0.46	0.0212	0.0425	0.0637
SPH 3.1 (Ø5)	31.14	4.36	0.39	0.0211	0.0423	0.0634
SPH 1.2 (Ø10)	33.15	3.43	0.32	0.0239	0.0477	0.0716
SPH 2.2 (Ø10)	32.31	3.17	0.50	0.0230	0.0460	0.0691
SPH 3.2 (Ø10)	31.68	3.74	0.46	0.0215	0.0429	0.0644
SPH 1.3 (Ø15)	33.54	3.42	0.41	0.0251	0.0501	0.0752
SPH 2.3 (Ø15)	35.07	2.80	0.48	0.0283	0.0566	0.0849
SPH 3.3 (Ø15)	31.29	3.58	0.60	0.0274	0.0549	0.0823
Mean value	31.64	3.78	0.45	0.0239	0.0477	0.0716
	Proposed value for Form error:			0.0477	0.0955	0.1432

These distance values should be understood as the values of the half-interval that defines the point-cloud form error once spurious points (outliers) have been removed. This definition could be valid for point clouds obtained by laser scanning or other non-contact reverse engineering equipment.

The value of the distance from which points are removed reflects low dispersion for each type of filter independently of the sphere and its diameter (average values are 0.0239 mm for 1σ filter, 0.0477 mm for 2σ filter and 0.0716 mm for 3σ filter). The intervals ±1σ, ±2σ, ±3σ are 0.0477, 0.0955 and 0.1432 mm, respectively (Table 3). The ±2σ and ±3σ intervals can be used to obtain with a good level of approximation the form error of laser measured point-clouds whereas the ±1σ filter provides unrealistic values, since the reference value (measured by contact) for the form error is always greater than 0.0711 mm (sphere 2.2, see Fig. 10 (b)).

7. Conclusions

This paper presents a study on the suitability of a laser line sensor for the metrological control of parts manufactured by SLM additive manufacturing process. At the same time, the capacity of the SLM process itself to manufacture accurately sphere-type geometric characteristics is evaluated. For this purpose, a test artifact has been designed which consists of a series of spheres, which are entities with a complete and simple metrological characterization. Geometrically and dimensionally, the test artifact allows, on the one hand, an optimal measurement with state-of-the-art line laser equipment and, on the other hand, it optimally covers the working space of the 3D metal printer.

Based on this special design, the part is printed on metal and then sandblasted. Both processes correctly emulate the usual work with this type of technology. For the research, the spheres were measured with high density scans, first by contact probing (CMM), and then by laser scanning. The measurement by

contact was made in initial conditions (as-built) and after the sandblasting process. The former already offered interesting data such as the SLM process produces spheres of less diameter (between -0.1038 and -0.1356 mm) than the nominal one (CAD model), and with high form errors (over 0.10 mm). Naturally, the post-sandblasting measures offered diameter values even further away from the nominal (-0.1563 to -0.1861 mm) due to the material removal. In any case, these last measurements will be the reference measurements for the subsequent study, comparing the contact with the laser equipment measurements.

The comparison of contact measurement results at different stages of the process (as-built and post sandblasting) provides very interesting data about the rate of erosion caused by sandblasting, a rate that mainly affects the diameter of the spheres, but also to their form error. It has been verified that, from the dimensional point of view, the erosion rate caused by sandblasting is practically constant and independent of the diameters and the positions of the spheres on the plate, in the order of 0.05 mm. The results of this analysis may be taken into account for modifying the CAD design of a sphere in order to improve its dimensional accuracy. Regarding the spheres form error, sandblasting also resulted in a greater uniformity, with values close to 0.08 mm.

With regard to the measurements performed with the laser sensor, it should be noted that a previous study was carried out to find the best scanning strategy, balancing the capture of an adequate number of points and a good coverage of the surface to scan. The optimal strategy involves covering the whole upper hemisphere, with 5 different passes that included the whole artifact (each sphere was scanned in 5 orientations). Then point clouds obtained from each sphere were trimmed below the equator, obtaining diameters (from the best fit spheres) and form errors. Laser sensor measurements of the SLM printed part provided different values with respect to contact measurement. In general, worse values were obtained for diameters, which were even farther (0.1 mm) from the reference values, and for the form error, being the difference in this case up to 0.2 mm with regard the form error measured by contact. It is obvious that, in parts manufactured by the SLM process, the generated surface present specific particularities, such as the variability of the normal vectors at closer points of the surface or the corresponding brightness, which causes the appearance of spurious points during the scanning, thus increasing the measurement errors when this technology is employed.

This work proposes the use of the standard deviation of the point cloud as a parameter to measure the form error of entities created by laser point clouds. For this purpose, it is necessary to use filters that remove specifically those points that are largely responsible of the difference between the measured values and the reference ones. After analysing the filters available in various software applications, it was concluded that using the filter based on the point cloud standard deviation is the best solution. This is a filter that almost all software packages implement producing similar results. Specifically, the filter that removes points located at a distance (from the surface boundary) greater than twice the standard deviation (2σ) is the filter that provides closer values to the actual reference form errors of the best fit entities. The filter of 3σ removes less points while maintains more information about the geometry, although it provides values already a little farther away from the reference form error.

In summary, for the surfaces obtained by SLM and sandblasting, results that better match the reference values measured by contact are obtained when a 2σ filter is applied. On the other hand, 3σ filter is expected to be suitable for scanning other canonical entities, such as planes, cylinders, or cones, were the better reflection conditions produces less noisy points. Nevertheless, these aspects must be studied in a future work. Finally, the third 1σ filter should not be employed as it removes an excessive number of points thus distorting the measurements. These results are very important for using this type of scanning technology when applied to 3D metal printing, process that is not an isolated technology and needs to be brought into a workflow, with steps like part design, part printing, post-processing and inspection.

Acknowledgements

Authors thank to the financial support provided by the Junta de Castilla y León (project LE027P17-FEDER funds) and also to two student grants awarded by the University Institute of Industrial Technology of

Asturias (IUTA, ref. SV-19-GIJON-1-14) and by the Young researcher mobility program of SIF (Manufacturing Engineering Spanish Society).

References

[1] Martinez S, Cuesta E, Barreiro J, Alvarez BJ. Analysis of laser scanning and strategies for dimensional and geometrical control. Int J of Adv Manuf Technol 2010;46(5):621–29. doi:10.1007/s00170-009-2106-8

[2] Bešić I, Van Gestel N, Kruth J-P, Bleys P, Hodolic J. Accuracy improvement of laser line scanning for feature measurements on CMM. Opt Lasers Eng 2011;49:1274–80. doi:10.1016/j.optlaseng.2011.06.009

[3] Isheil A, Gonnet J-P, Joannic D, Fontaine J-F. Systematic error correction of a 3D laser scanning measurement device. Opt Lasers Eng 2011;49:16–24. doi:10.1016/j.optlaseng.2010.09.006

[4] MacKinnon D, Carrier B, Beraldin J-A, Cournoyer L. GD&T-based characterization of short-range non-contact 3D imaging systems. Int J of Comput Vis 2013;102(1-3):56–72. doi:10.1007/s11263-012-0570-3

[5] Rak M, Woźniak A. Systematic errors of measurements on a measuring arm equipped with a laser scanner on the results of optical measurements. In: Jabłoński R., Brezina T. (eds) Advanced Mechatronics Solutions. Advances in Intelligent Systems and Computing, vol 393. Springer, Cham, 2016. doi:10.1007/978-3-319-23923-1_54

[6] ISO 10360-7 (2011) Geometrical product specifications (GPS)—Acceptance and re-verification tests for coordinate measuring machines (CMM)—Part 7: CMMs equipped with imaging probing systems. International Organization for Standardization, Geneva

[7] VDI/VDE 2634-1,2,3 (2002) Optical 3D measuring systems—imaging systems with point-by-point probing. VDI, Beuth, Berlin

[8] The Association of German Engineers 2002 Optical 3D-measuring systems—optical systems based on area scanning VDI/VDE 2634 part 2

[9] Beraldin JA, Mackinnon D, Cournoyer L. Metrological characterization of 3D imaging systems: progress report on standards developments. In 17th International Congress of Metrology 2015 (p. 13003). EDP Sciences. doi:10.1051/metrology/20150013003

[10] Acko B, McCarthy M, Haertig F, Buchmeister B. Standards for testing freeform measurement capability of optical and tactile coordinate measuring machines. Meas Sci Technol 2012;23(9):094013. doi:10.1088/0957-0233/23/9/094013

[11] McCarthy MB, Brown SB, Evenden A, Robinson AD. NPL freeform artifact for verification of non-contact measuring systems. In Three-Dimensional Imaging, Interaction, and Measurement 2011 Jan 27 (Vol. 7864, p. 78640K). International Society for Optics and Photonics. doi:10.1117/12.876705

[12] Iuliano L, Minetola P, Salmi A. Proposal of an innovative benchmark for comparison of the performance of contactless digitizers. Meas Sci and Technol 2010;21(10):105102. doi: 10.1088/0957-0233/21/10/105102

[13] Gonzalez-Jorge H, Riveiro B, Armesto J, Arias P. Standard artifact for the geometric verification of terrestrial laser scanning systems. Opt Lasers Eng 2011;43(7):1249–56. doi: 10.1016/j.optlastec.2011.03.018

[14] MacKinnon D, Carrier B, Beraldin JA, Cournoyer L. GD&T-based characterization of short-range non-contact 3D imaging systems. Int J of Comput Vis 2013;102(1-3):56–72. doi: 10.1007/s11263-012-0570-3

[15] Farooqui SA, Morse EP. Methods and Artifacts for Comparison of Scanning CMM Performance. J Comput Inf Sci Eng 2007; 7(1): 72–80. doi:10.1115/1.2709928

[16] Cuesta E, Rico JC, Fernandez P, Blanco D, Valiño G. Influence of roughness on surface scanning by means of a laser stripe system. Int J Adv Manuf Technol 2009;43(11-12):1157–66. doi: 10.1007/s00170-008-1794-9

[17] Wang Y, Feng HY. Modeling outlier formation in scanning reflective surfaces using a laser stripe scanner. Measurement 2014;57:108–21. doi: 10.1016/j.measurement.2014.08.010

[18] Wang Y, Feng HY. Effects of scanning orientation on outlier formation in 3D laser scanning of reflective surfaces. Opt Lasers Eng 2016;81:35–45. doi: 10.1016/j.optlaseng.2016.01.003

[19] Rak M, Woźniak A. The influence of properties of a measured object on the surface digitalization performed by a laser scanner integrated with measuring arm. Pomiary Automatyka Robotyka 2012;12:76–81. doi:

[20] Mendricky R, Langer O. Influence of the material on the accuracy of optical digitalization. MM Science Journal 2019;I:2783–89. doi:10.17973/MMSJ.2019_03_2018121

[21] Van Gestel N, Cuypers S, Bleys P, Kruth JP. A performance evaluation test for laser line scanners on CMMs. Opt Lasers Eng 2009;47(3-4):336–42. doi:10.1016/j.optlaseng.2008.06.001

[22] Bešić I, Van Gestel N, Kruth JP, Bleys P, Hodolič J. Accuracy improvement of laser line scanning for feature measurements on CMM. Opt Lasers Eng 2011;49(11):1274–80. doi: 10.1016/j.optlaseng.2011.06.009

[23] Boeckmans B, Probst G, Zhang M, Dewulf W, Kruth JP. ISO 10360 verification tests applied to CMMs equipped with a laser line scanner. In Dimensional Optical Metrology and Inspection for Practical Applications V 2016 May 19 (Vol. 9868, p. 986805). International Society for Optics and Photonics. doi:10.1117/12.2227061

[24] Mahmud M, Joannic D, Roy M, Isheil A, Fontaine JF. 3D part inspection path planning of a laser scanner with control on the uncertainty. Comput Aided Des 2011;43(4):345–55. doi:10.1016/j.cad.2010.12.014

[25] Satyanarayana A, Krishna M, Chandrakanth A, Pradyumna R. Influence of LASER CMM Process Parameters on Dimensional Inspection of Standard Spheres. Materials Today: Proceedings 2018;5(2):3965–70. doi:10.1016/j.matpr.2017.11.654

[26] Rad M, Woźniak A, Mayer JR. The influence of the scanning path of a laser scanner integrated with measuring arm on the surface digitalization. In Proceedings of the tenth International Scientific Conference Coordinate Measuring Technique 2012, Bielsko-Biała -Ustron, Poland. doi:10.13140/2.1.2115.9045

[27] Cuesta E, Alvarez BJ, Martinez-Pellitero S, Barreiro J, Patiño H. Metrological evaluation of laser scanner integrated with measuring arm using optical feature-based gauge. Opt Lasers Eng 2019;121:120–32. doi:10.1016/j.optlaseng.2019.04.007

[28] Gerbino S, Del Giudice DM, Staiano G, Lanzotti A, Martorelli M. On the influence of scanning factors on the laser scanner-based 3D inspection process. Int J Adv Manuf Technol 2016;84(9-12):1787–99. doi: 10.1007/s00170-015-7830-7

[29] Ratajczyk E, Rak M, Kowaluk T. The influence of method of points collection on results with the use of measuring arm. Metrol Meas Syst 2012;19(3):541–52. doi: 10.2478/v10178-012-0047-2

[30] Guerra MG, De Chiffre L, Lavecchia F, Galantucci LM. Use of miniature step gauges to assess the performance of 3D optical scanners and to evaluate the accuracy of a novel additive manufacture process. Sensors 2020;20(3):738. doi:10.3390/s20030738

[31] Barbero BR, Ureta ES. Comparative study of different digitization techniques and their accuracy. Comput Aided Des 2011;43(2):188–206. doi:10.1016/j.cad.2010.11.005

[32] Palousek D, Omasta M, Koutny D, Bednar J, Koutecky T, Dokoupil F. Effect of matte coating on 3D optical measurement accuracy. Opt Mater 2015;40:1–9. doi:10.1016/j.optmat.2014.11.020

[33] Craeghs T, Clijsters S, Yasa E, Kruth JP. Online quality control of selective laser melting. In Proceedings of the 20th Solid Freeform Fabrication (SFF) symposium, Austin (Texas), 8-10 august 2011 (pp. 212–226).

[34] Craeghs T, Bechmann F, Berumen S, Kruth JP. Feedback control of Layerwise Laser Melting using optical sensors. Phys Procedia 2010;5:505–14. doi:10.1016/j.phpro.2010.08.078

[35] Leach R, Haitjema H, Giusca C. A metrological characteristics approach to uncertainty in surface metrology. In: Osten W, editor. Optical Inspection of Microsystems, Boca Raton: CRC Press; 2019; p. 73–92. doi:10.1201/9780429186738-3

[36] Thompson A, Maskery I, Leach RK. X-ray computed tomography for additive manufacturing: a review. Meas Sci Technol 2016;27(7):072001. doi:10.1088/0957-0233/27/7/072001

[37] Villarraga-Gomez H, Lee C, Smith ST. Dimensional metrology with X-ray CT: A comparison with CMM measurements on internal features and compliant structures. Precis Eng 2018;51:291–307. doi:10.1016/j.precisioneng.2017.08.021

[38] Stavroulakis PI, Leach RK. Invited Review Article: Review of post-process optical form metrology for industrial-grade metal additive manufactured parts. Rev Sci Instrum 2016;87(4):041101. doi:10.1063/1.4944983

[39] Udroiu R, Braga IC, Nedelcu A. Evaluating the Quality Surface Performance of Additive Manufacturing Systems: Methodology and a Material Jetting Case Study. Materials 2019;12(6):995. doi:10.3390/ma12060995

[40] Su X, Yang Y. Research on track overlapping during selective laser melting of powders. J Mater Process Technol 2012;212(10):2074-9. doi:10.1016/j.jmatprotec.2012.05.012

[41] Yadroitsev I, Gusarov A, Yadroitsava I, Smurov I. Single track formation in selective laser melting of metal powders. J Mater Process Technol 2010;210(12):1624–31. doi:10.1016/j.jmatprotec.2010.05.010

[42] Townsend A, Senin N, Blunt L, Leach RK, Taylor JS. Surface texture metrology for metal additive manufacturing: a review. Precis Eng 2016;46:34–47. doi:10.1016/j.precisioneng.2016.06.001

[43] Dowling L, Kennedy J, O'Shaughnessy S, Trimble D. A review of critical repeatability and reproducibility issues in powder bed fusion. Mater Design 2020;186:108346. doi:10.1016/j.matdes.2019.108346

[44] Everton SK, Hirsch M, Stravroulakis P, Leach RK, Clare AT. Review of in-situ process monitoring and in-situ metrology for metal additive manufacturing. Mater Design 2016;95:431–45. doi:10.1016/j.matdes.2016.01.099

[45] Bagehorn S, Mertens T, Greitemeier D, Carton L, Schoberth A. Surface finishing of additive manufactured ti-6al-4v–a comparison of electrochemical and mechanical treatments. In 6th European Conference for Aeronautics and Space Sciences (EUCASS 2015), Kraków, Poland, 2015.

[46] Cuesta E, Gonzalez-Madruga D, Alvarez BJ, García-Dieguez M. Development of a behaviour curve for quality evaluation with optoelectronic profilometers. In: Key Engineering Materials 2014 (Vol. 615, pp. 51-56). Trans Tech Publications Ltd. doi:10.4028/www.scientific.net/KEM.615.51

[47] Cuesta E, Gesto A, Alvarez BJ, Martínez-Pellitero S, Zapico P, Giganto S. Dimensional accuracy analysis of Direct Metal Printing machine focusing on roller positioning errors. Procedia Manuf 2019;41:2–9. doi:10.1016/j.promfg.2019.07.022

[48] Zapico P, Giganto S, Martínez-Pellitero S, Fernandez-Abia M I, Castro-Sastre MÁ. Influence of Laser Energy in the Surface Quality of Parts Manufactured by Selective Laser Melting. Annals of DAAAM & Proceedings 2018;29:0279–86. doi:10.2507/29th.daaam.proceedings.040

[49] ISO 1101:2017. Geometrical product specifications (GPS) - Geometrical tolerancing - Tolerances of form, orientation, location and run-out; 2017.